ARTICLE

Check for updates

Sustained coral reef growth in the critical wave dissipation zone of a Maldivian atoll

Paul S. Kench [1✉], Edward P. Beetham[2], Tracey Turner[3], Kyle M. Morgan [4,5], Susan D. Owen[6] & Roger. F. McLean[7]

Sea-level rise is expected to outpace the capacity of coral reefs to grow and maintain their wave protection function, exacerbating coastal flooding and erosion of adjacent shorelines and threatening coastal communities. Here we present a new method that yields highly-resolved direct measurements of contemporary reef accretion on a Maldivian atoll reef rim, the critical zone that induces wave breaking. Results incorporate the suite of physical and ecological processes that contribute to reef accumulation and show growth rates vary from 6.6 ± 12.5 mm.y^{-1} on the reef crest, and up to 3.1 ± 10.2 mm.y^{-1}, and -0.5 ± 1.8 mm.yr^{-1} on the outer and central reef flat respectively. If these short-term results are maintained over decades, the reef crest could keep pace with current sea-level rise. Findings highlight the need to resolve contemporary reef accretion at the critical wave dissipation zone to improve predictions of future reef growth, and re-evaluate exposure of adjacent shorelines to coastal hazards.

[1] Department of Earth Sciences, Simon Fraser University, Burnaby, Canada. [2] Tonkin and Taylor International Ltd, Auckland, New Zealand. [3] School of Environment, University of Auckland, Auckland, New Zealand. [4] Asian School of the Environment, Nanyang Technological University, Singapore 637459, Singapore. [5] Earth Observatory of Singapore, Nanyang Technological University, Singapore, Singapore. [6] School of Resource and Environmental Management, Simon Fraser University, Burnaby, Canada. [7] School of Science, University of New South Wales-Canberra, Canberra, ACT, Australia. ✉email: pkench@sfu.ca

Reduced coral reef growth capacity, as a consequence of global climatic change and anthropogenic stressors, poses a major threat to reef-fronted coastal communities[1–7]. Modelling studies suggest that tropical coral reefs serve as natural protective barriers to incident ocean wave energy, reducing coastal hazard risks along reef-fringed coastlines[1,3]. In Indo-Pacific reef settings this protective function is primarily dependent on the elevation of the reef edge with respect to sea level, which induces breaking of incident ocean waves in shallow water at the reef crest. Further dissipation and transformation of residual wave energy that impacts shorelines is also dependent on relative water depth and width of the reef flat (Fig. 1). The presence of the reef structure and the associated protective functions it provides shorelines, relies on the net accumulation of calcium carbonate material by living reef ecological communities, which when consolidated in the reef framework, contributes to vertical reef accretion. The potential for net accumulation at any point in time represents the balance of constructive (e.g. calcification by living corals, coralline algae and other calcifiers) and erosive (e.g. bioerosion, chemical dissolution and physical) processes[8]. Consequently, the elevation of existing reef structures reflects the culmination of cycles of growth, decay, and hiatus as the balance of these competing constructive and destructive forces shifted in response to changing environmental conditions across geological timescales.

During the Holocene (past 10,000 years), reef growth rates have been shown to vary between 1 and 20 mm.yr^{-1} due to differences in both sea level histories and ecological legacies deriving from the productivity and composition of past reef communities[9]. The ecological condition and capacity of contemporary reefs to maintain existing, or support future, vertical growth is uncertain. Sea-level rise is expected to reduce the protective function of reefs, as increased water depths across reef surfaces open the wave energy window, and exacerbate shoreline erosion and flooding of coastal communities[3,7,10,11]. Increases in relative water depth across reefs will occur where rates of vertical reef growth lag behind rates of sea-level rise, and where degradation of the reef surface through coral mortality, and physical and biological breakdown processes reduce the level of the reef flat[12,13]. In these instances there may be increases in the magnitude of wave energy that reaches adjacent shorelines[13]. This relative reef submergence hypothesis, and increase in hazard risk to coastal communities, has assumed widespread acceptance[3,5,14] given current scenarios of sea-level rise of 0.44 m (RCP 2.6) to 0.75 m (RCP 8.5) by 2100[15,16], and declines in the global abundance and productivity of tropical reef-building corals that drive vertical reef growth potential[4,17–20]. Here we present an important contribution to understanding contemporary and future coral reef growth potential and the role of reefs in acting as wave protection structures as it: (1) introduces a method to directly quantify rates of reef growth; (2) presents new data of contemporary reef growth from the critical wave breaking zone of an Indo-Pacific oceanic atoll, and; (3) uses these contemporary measurements to consider future reef growth to maintain wave protective functions for coastal resilience. The findings challenge prevailing interpretations of reef growth that are largely derived from submerged fore-reef settings and provide both conceptual and methodological advances in the approach to future analyses of reef growth potential.

While projections of future rates of sea-level rise continue to be refined, the greenhouse commitment will ensure substantive increases in sea level are locked into the climate-ocean system for several centuries[21–23]. In contrast, estimates of contemporary and future reef growth performance are less well constrained and can be expected to exhibit marked geographic variation[4,24]. Studies of paleo-reef growth have typically been assessed using geological reconstructions from reef cores[9,25–27]. However, such paleo-reconstructions are considered to have limited value in evaluating
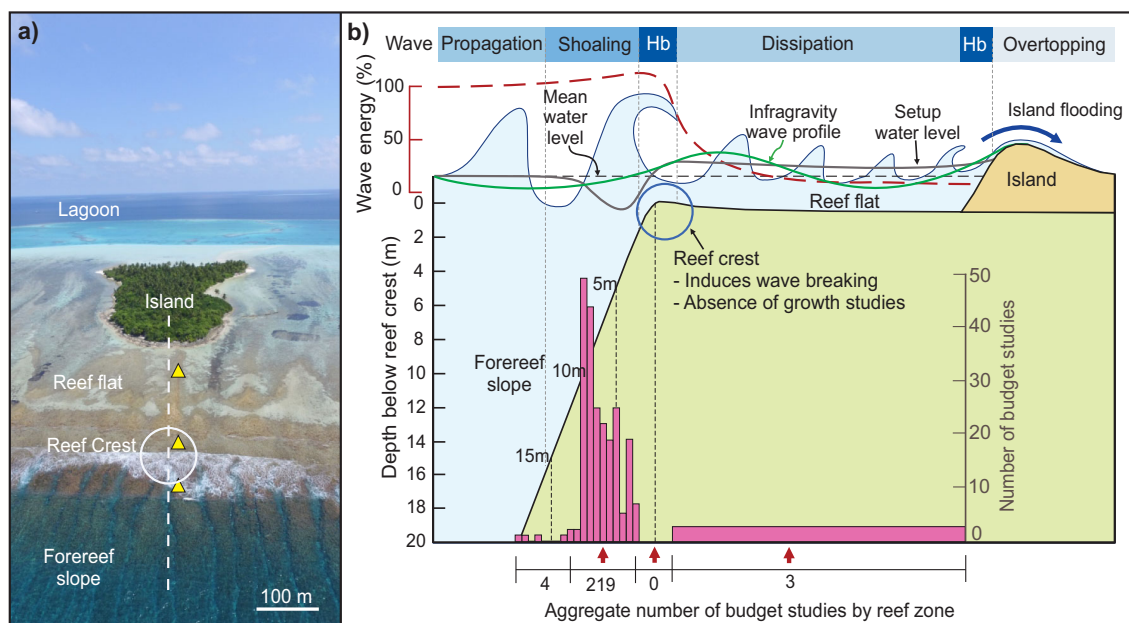

Fig. 1 Summary of wave interactions with Indo-Pacific coral reefs and reef flats. a Field location on the southwest rim of Huvadhoo atoll, Maldives, central Indian Ocean, showing primary geomorphic components of reef structure (also see Methods and Supplementary Fig. 1). Dashed line represents profile presented in **b**. Yellow triangles show the location of wave gauges used to document cross-reef reduction in wave energy of 90% presented in Supplementary Fig. 2. **b** Summary of wave process interactions with a coral reef. The reef crest induces critical wave breaking (Hb) and cross-reef reduction in energy with subsequent cross-reef flat wave transformations that can promote island flooding under higher wave energy conditions. Note the spatial distribution of contemporary carbonate budget studies by depth and the concentration of budget studies on forereefs at depths of 7–10 m which are used as proxies for potential vertical reef growth, and the paucity of reef growth estimates for the reef crest and reef flat (data sources for budget studies presented in Supplementary Data 1).

current and future reef growth capacity as the start-up and growth conditions (e.g., water quality, depth, chemistry) of reef communities in the Holocene are thought to differ markedly to those of present-day reef systems[24]. Due to the slow growth rates of reef calcifying organisms, and the extended duration of investigations needed to detect changes in reef surface elevation, there have been few attempts to undertake direct measurements of contemporary reef growth. To date, estimates of contemporary rates of reef growth have largely relied on indirect census-based observations of living cover and their subsequent conversion to growth rates. In particular, studies based on in-situ ecological surveys have estimated the net carbonate budget state of reefs[28–30]. These datasets have also been used to derive first-order estimates of vertical reef growth potential, ranging from -0.84 to 4.0 mm yr^{-1}[, 28], and subsequently to assess the possible magnitude of reef submergence with future sea-level rise[4]. Results of these studies have shown marked regional differences in potential reef growth, partly driven by the scale of recent mass coral bleaching events within defined ecoregions, and have highlighted the susceptibility of reef growth rates to temporal shifts in ecological state[4,20].

While these studies have yielded valuable insights into the carbonate budget state and budget dynamics of modern reefs, their value in estimating vertical reef growth, possible reef submergence and, therefore, changes in coastal hazard risk is limited. First, the studies invoke assumptions in converting net calcium carbonate deposition in Kg.m^{-2}.yr^{-1}(G) to linear reef accretion (mm.yr^{-1}) that remain poorly validated. Second, the role of detrital sediment generation and its subsequent offreef export or redeposition within the reef matrix is not directly assessed, potentially under-representing rates of reef accumulation[31]. Third, and most significantly for resolving the problem of reef flat submergence, data underpinning carbonate budget studies and estimates of rates of contemporary reef growth are gathered from reef zones that are peripheral to the reef crest, which is the critical area of wave breaking and dissipation that modulates shoreline hazards (Fig. 1). Constrained by field logistics, the majority of budget studies have been undertaken on less energetic and deeper fore-reef slopes that are accessible by SCUBA (Fig. 1b). While driven by discrete research questions of broader reef ecosystem health, studies from these deeper locations are of lesser importance in understanding the role of the reef to modulate wave energy in Indo-Pacific reef settings, compared to the shallow reef crest and outer reef flats, the critical geomorphic zones of a reef that control the dissipation and transmission of wave energy to adjacent shorelines. Fourth, reef crest zones, particularly in the Indo-Pacific, are commonly comprised of distinct calcifying communities (e.g. wave resistant coral morphotypes and crustose coralline algae) that drive reef growth in these critical wave stress zones, and these communities may respond differently, compared with deeper forereef counterparts, to major disturbance events because of the greater water exchange and wave stresses at shallow depths.

Depth-limited wave breaking occurs in proximity of the reef crest in Indo-Pacific reef flat settings and it is this process, combined with subsequent transformations of residual energy across reef flats, that is important in determining wave inundation and erosion potential of coastlines (Fig. 1b, Supplementary Fig. 2). This relationship is evident in the inclusion of reef depth as a primary variable when developing empirical relationships to describe wave energy reduction on coral reefs[7,32]. Consequently, it is the growth performance of the reef crest and outer reef flat that are vital in evaluating changes in the role of reefs in transforming oceanic wave energy. Recognition that the ecological composition and morphological structure of the reef crest and reef flat are markedly different to the forereef environment

suggests the growth potential and response to external disturbance events of these key geomorphic zones are also likely to differ[33]. Such differences are significant as reductions in growth of the reef crest can influence whether waves break or propagate onto the reef surface, whereas changes in accretion of the forereef[4,26] may only induce minor modification to wave shoaling processes (Fig. 1b). As has been shown by Roff[26], where accommodation space is available on reef slopes reefs can accrete at rates equal to or exceeding that of the mid-Holocene climatic optimum. In contrast, few studies have examined the productive capacity of reef crest environments[34–36], or generated contemporary growth rate estimates of exposed reef crests and adjacent ocean reef flats (Fig. 1b).

Here we present a direct measurement approach that utilises coral reef accretion frames (CRAFs) to make highly-resolved and repeatable measurements of changes in reef surface topography at four locations across the reef crest and outer reef flat of Huvadhoo atoll in the southern Maldives, central Indian Ocean (see Methods, Supplementary Fig. 1). Coral reef accretion monitoring (CRAM) sites spanned the first 65 m of the reef crest and outer reef flat, the zone critical to inducing wave breaking processes on coral reefs (Supplementary Fig. 1c,d). The CRAM sites were selected to ensure coverage of the different eco-geomorphic zones including the crustose coralline algae (CCA) dominated reef crest, the mixed CCA and coral zone on the outer reef flat, and algal pavement on the central reef flat (Supplementary Note 1, Supplementary Fig. 3, Supplementary Tables 1 and 2). Notably, our reef crest sites represent a modern analogue of the coralline algal reef framework facies common to Indo-Pacific reef crest environments as determined through geological core analysis[9]. Our high-resolution measurements were repeated annually over a three-year timeframe (2018–2020) and integrate the suite of physical and ecological processes that contribute to reef accretion and erosion at the CRAM sites. This study commenced approximately 18 months after the third global coral bleaching event affected the central Indian Ocean in 2016, with studies reporting significant declines in live coral cover at nearby reef sites in the southern Maldives, including Huvadhoo atoll[37,38]. Monitoring results of reef surface topographic change are examined in the context of processes governing reef flat accretion and current and future scenarios of sea level change.

Results

Measurements indicate the CRAFs are able to detect micro-scale changes in surface elevation between consecutive years and show the reef flat surface has a dynamic topography at the millimetre to sub-metre scale (Fig. 2, Table 1, Supplementary Figs. 4–7 and Supplementary Data 2). There was a statistically significant difference in the measured changes in reef surface elevation (mm) for the two-year observational period between CRAM sites (one way Kruskal-Wallis test, $H(3) = 521$, $p = 0.0001$). Pairwise post-hoc tests (Dunn test with Bonferroni adjustments) indicate the measured differences in reef surface elevation change (mm) were significant between all four CRAM sites (Supplementary Table 3). At the CCA and encrusting coral-dominated reef crest zone, results identify a net increase in reef elevation of 13.2 mm across the two-year observational period at a mean annual rate of 6.6 ± 12.6 mm.y^{-1}. The reef crest site showed consistent annual net accretion with values of 5.4 ± 20.4 mm.y^{-1} and 7.8 ± 15.8 mm.y^{-1} for 2019 and 2020 respectively (Fig. 2a, Supplementary Fig. 4). These aggregated site values mask intra-plot variability in elevation change, between the 7 measurement transects within the CRAM plot, that range from -10.6 ± 27.8 mm.y^{-1} (CS1-Transect A in 2019, Table 1) to 17.0 ± 20.0 mm.y^{-1} (CS1-Transect N1 in 2020, Table 1). Notably 93% of transects displayed net accretion. Within the entire plot
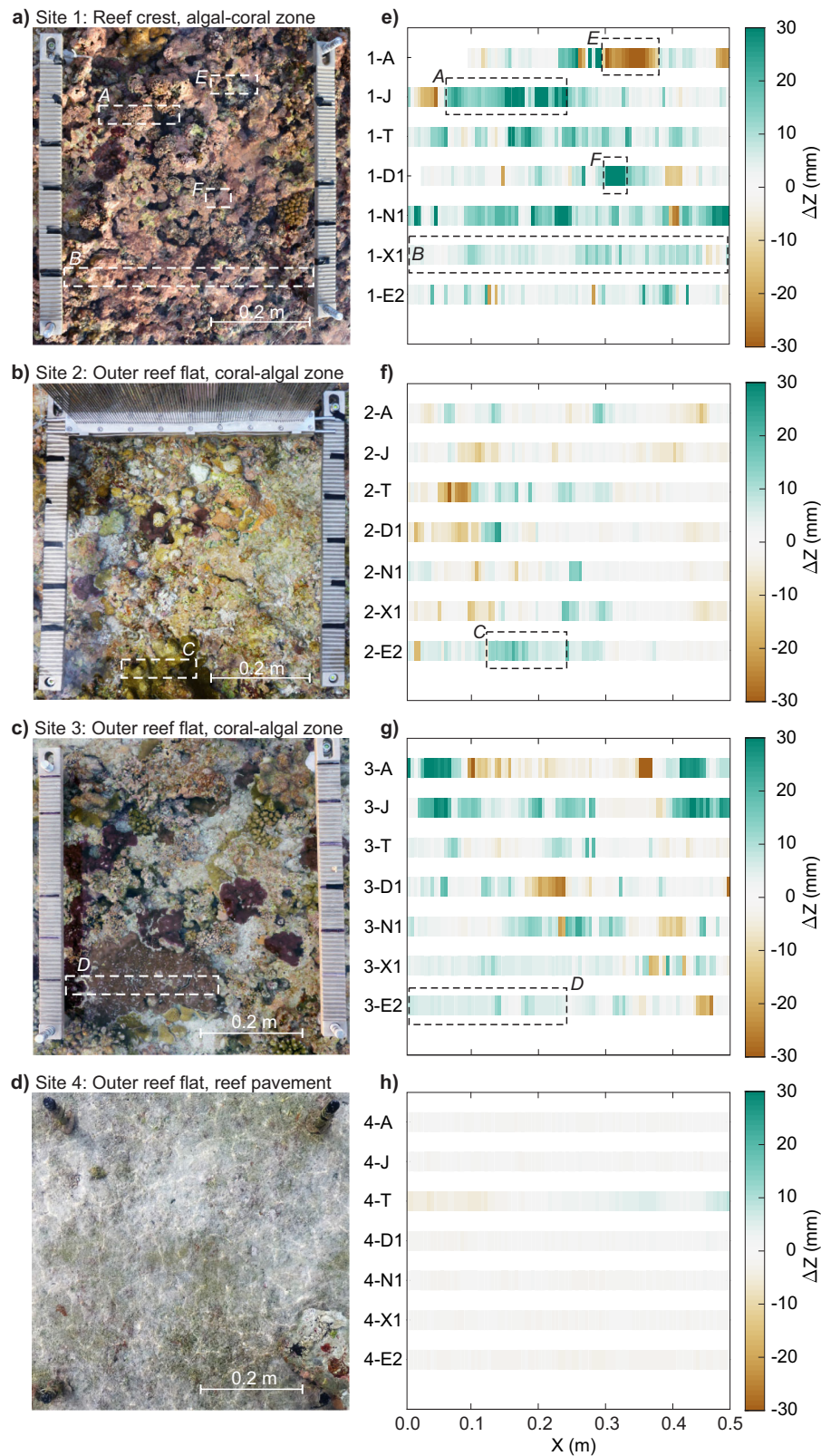
Fig. 2 Summary results of reef topographic change at CRAM sites, Keleihutta reef flat, Maldives. a–d show images of each CRAM site. **c–h** Present corresponding summaries of topographic change across the two year experiemntal period, along each of 7 transect lines (A, J, T, D1, N1, X1, and E2). Individual transect lines presented in Supplementary Figs. 4–7. Inset boxes are areas highlighted in Fig. 3.

dataset (1,386 points) point-scale variation ranged from a maximum of 134.8 mm to −92.0 mm in a single year.

CRAM sites 2 and 3 were both located on the outer reef flat in the coral-algal zone. Site 2 showed minimal net surface change

across the measurement period $−0.07 ± 6.1$ mm.y^{-1} and this value was consistent across both measurement years (Table 1). Despite the negligible net change individual transect results ranged from $−6.5 ± 10.4$ mm.y^{-1} to $6.0 ± 8.8$ mm.y^{-1} with

Table 1 Summary changes in reef surface elevation at Coral Reef Accretion Monitoring (CRAM) sites.

CRAM Site	Transect	2018–19 (mm/yr)	2019–20 (mm/yr)	Tot. Change 2018–20 (mm)	Tot. Change 2018–20 (mm/y)	Max (mm/yr)	Min (mm/yr)
CS1. Reef crest	A	−10.6 ± 27.8	5.1 ± 22.5	−5.5 ± 35.9	−2.8 ± 18.0	128.5	−78.1
	J	7.9 ± 21.2	11.2 ± 14.5	19.1 ± 27.5	9.54 ± 13.8	95.0	−55.5
	T	9.4 ± 19.6	8.2 ± 7.9	17.2 ± 21.2	8.6 ± 10.6	134.8	31.8
	D1	7.7 ± 25.7	3.9 ± 15.3	11.6 ± 27.4	5.8 ± 13.7	110.2	−92.0
	N1	8.8 ± 18.9	17.0 ± 20.0	25.8 ± 22.9	12.9 ± 11.5	76.5	−49.3
	X1	4.6 ± 7.5	7.3 ± 6.6	11.9 ± 9.3	6.0 ± 4.7	30.2	−20.2
	E2	6.9 ± 9.7	1.0 ± 13.1	7.9 ± 14.2	4.0 ± 7.1	48.1	−85.1
	Mean	5.4 ± 20.4	7.8 ± 15.8	13.2 ± 25.2	6.6 ± 12.6	134.8	−92.0
CS2. Outer reef flat: coral-algal zone	A	−0.9 ± 8.2	1.7 ± 13.3	0.8 ± 10.3	0.4 ± 5.2	49.9	−30.8
	J	1.7 ± 11.8	−6.5 ± 10.4	−4.9 ± 7.7	−2.5 ± 4.0	30.6	−31.8
	T	0.2 ± 14.7	−0.7 ± 12.2	−0.5 ± 16.9	−0.3 ± 8.5	38.5	−44.1
	D1	−4.1 ± 13.3	1.1 ± 8.8	−2.9 ± 12.5	−2.5 ± 6.3	39.0	−46.7
	N1	−0.3 ± 6.3	0.4 ± 5.8	0.2 ± 9.0	0.1 ± 4.5	22.0	−26.9
	X1	1.5 ± 8.4	−2.5 ± 5.6	−1.0 ± 11.1	−0.5 ± 5.6	27.7	−25.3
	E2	1.5 ± 12.2	6.0 ± 8.8	7.4 ± 12.1	3.7 ± 6.1	37.6	−42.8
	Mean	−0.06 ± 11.2	−0.07 ± 10.3	−0.14 ± 12.2	−0.07 ± 6.1	49.9	−66.5
CS3. Outer reef flat: coral-algal zone	A	1.0 ± 27.8	1.5 ± 18.8	2.5 ± 34.3	1.3 ± 17.2	104.3	−96.0
	J	15.3 ± 19.4	5.1 ± 19.6	20.3 ± 20.9	10.2 ± 10.5	59.9	−39.2
	T	3.1 ± 9.1	−0.5 ± 6.9	2.5 ± 9.8	1.3 ± 4.8	42.4	−38.5
	D1	−1.9 ± 17.4	0.6 ± 9.7	−1.2 ± 18.6	−0.6 ± 9.3	57.9	−53.6
	N1	4.4 ± 14.5	1.8 ± 9.0	6.2 ± 16.7	3.1 ± 8.4	36.1	−52.3
	X1	−1.1 ± 15.6	8.2 ± 14.0	7.1 ± 11.1	3.5 ± 5.6	61.1	57.7
	E2	1.4 ± 7.6	3.9 ± 7.9	5.2 ± 12.2	2.6 ± 6.1	37.5	−31.4
	Mean	3.2 ± 17.8	2.9 ± 13.4	6.1 ± 20.3	3.1 ± 10.2	104.3	−96.0
CS4. Reef flat pavement zone	A	−1.4 ± 1.2	−0.2 ± 1.4	−1.6 ± 1.5	−0.8 ± 0.8	4.7	−4.2
	J	−1.5 ± 1.1	0.1 ± 1.3	−1.4 ± 1.3	−0.7 ± 1.2	3.7	−4.5
	T	0.4 ± 8.0	0.8 ± 1.3	1.2 ± 7.5	0.6 ± 3.8	16.8	−13.1
	D1	−1.4 ± 0.8	0.2 ± 1.6	−1.2 ± 2.0	−0.6 ± 1.0	4.6	−4.3
	N1	−2.3 ± 1.0	0.2 ± 1.3	−2.1 ± 1.8	−1.1 ± 0.9	4.0	−4.3
	X1	−1.9 ± 0.7	−0.6 ± 1.0	−2.6 ± 1.2	−1.3 ± 0.6	1.8	−3.7
	E2	−3.9 ± 1.1	4.6 ± 2.2	0.7 ± 2.2	0.35 ± 1.1	9.6	−6.0
	Mean	−1.7 ± 3.4	0.7 ± 2.2	−1.0 ± 3.5	−0.5 ± 1.8	16.8	−13.1

± values denote the standard deviation of measurements either in each transect (n = 99) or for all values in the plot (n = 693).

maximum and mimimum point-scale changes of 49.9 and −66.5 mm (Table 1, Fig. 2b, Supplementary Fig. 5). Site 3 showed a net reef surface accretion rate of 6.1 ± 20.3 mm across the study period at an annual rate of 3.1 ± 10.2 mm.y^{-1}. Annual net changes were 3.2 ± 17.8 mm.y^{-1} and 2.9 ± 13.4 mm.y^{-1} in 2019 and 2020 respectively (Table 1, Fig. 2c, Supplementary Fig. 6). At the transect scale, net change ranged from 15.3 ± 19.4 mm.y^{-1} to −1.9 ± 17.4 mm.y^{-1} with 78% of transects showing accretion. Point-scale variations ranged from 104.3 mm to −96.0 mm.

Results at the reef pavement location (CRAM Site 4) showed minor topographic change. Aggregated measurements at the plot scale suggest net change was −0.5 ± 1.8 mm.y^{-1}, within the margin of error of CRAF detection (Table 1, Fig. 2d, Supplementary Fig. 7). Annual net changes were −1.7 ± 3.4 mm.y^{-1} and 0.7 ± 2.2 mm.y^{-1} for 2019 and 2020 respectively. Within plot transect scale values of net surface, change ranged from 4.6 ± 2.2 mm.y^{-1} to −3.8 ± 1.1 mm.y^{-1}, with 57% of transects indicating minor surface lowering. Point-scale changes varied between 16.8 mm and −13.1 mm.

Discussion

We present direct quantitative measurements of contemporary changes in topography and net vertical accretion/growth of a coral reef crest and reef flat surface, the critical zone that induces wave breaking and dissipation in Indo-Pacific reef systems, and which afford protection to coastlines. Significantly our data, from a site in the Maldives where climate change induced sea-level rise

is expected to have significant implications, show the reef crest and outer reef flat surface is currently accreting, though there is considerable variability in net changes between CRAM sites that reflect ecological differences and, in particular, the proportion of living calcifiers. Notably our data show that the reef crest zone, dominated by coralline algae and encrusting corals, has accreted at a mean rate of 6.6 ± 12.6 mm.y^{-1} over a two-year period. Landward of this zone, the two measurement sites located in the coral algal zone showed differing responses, with negligible change at Site 2 and net accretion at Site 3 at ~3.1 ± 10.2 mm.y^{-1}, which is half the rate of growth recorded at the adjacent reef crest. Our most landward location (65 m from the reef crest) showed negligible change of the reef flat pavement surface, which is largely devoid of calcifiers and supports an epilithic algal matrix which encourages grazing and carbonate removal by reef herbivores. Measurements recorded at this location indicated that the reef surface under most transects exhibited minor surface lowering (mean net change of −0.5 ± 1.8 mm.y^{-1}) though within the measurement error. In general, our accretion rates are similar to those determined on experimental surfaces on reef crest and reef flat environments on St Croix, West Indies, with values up to 5.2 mm.y^{-1} and 0.5–1.0 mm.y^{-1} respectively[39]. Furthermore, the accretion rates for the reef crest (up to 6.6 mm.y^{-1}) and outer reef flat (up to 3.1 mm.y^{-1}) fall within the range reported for windward coralline algal-dominated framework facies during the Holocene, as derived from Indo-Pacific core records[9].

Aggregated CRAM plot results yield values of net vertical change in the reef surface that integrates the complex combination of
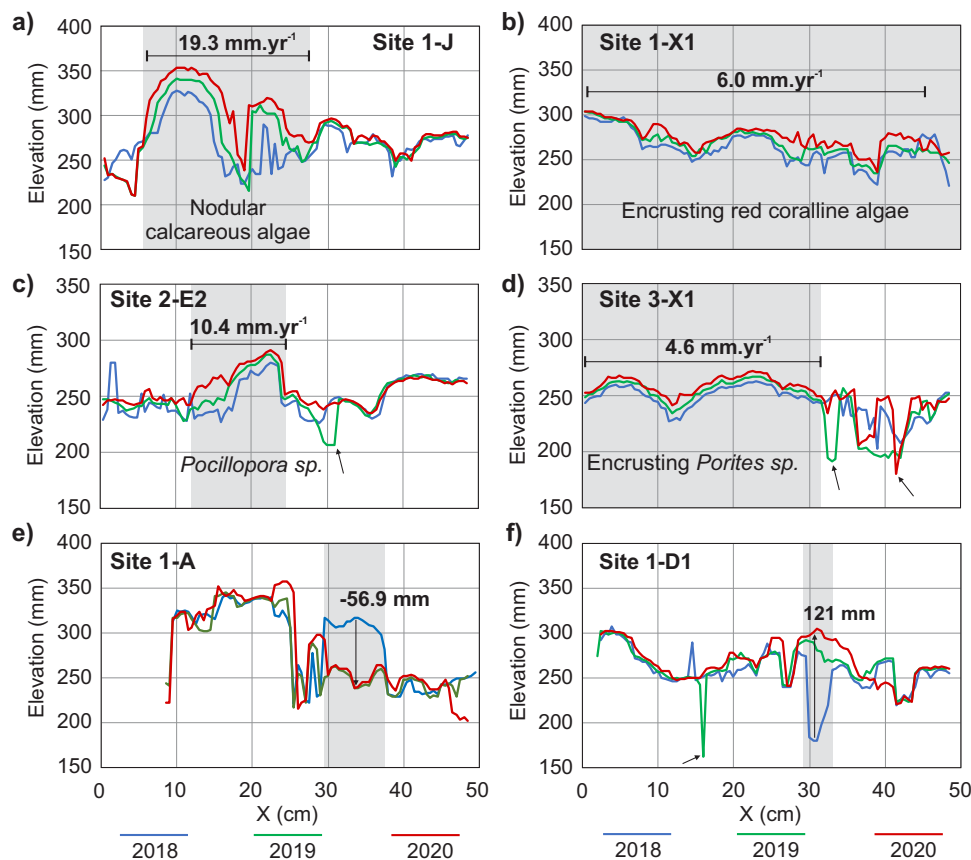
Fig. 3 Summary reef surface topographic change processes observed in coral reef accretion frame transects. a Nodular calcareous algae growth. **b** Incremental growth of encrusting red coralline algae-dominated transect. **c** Growth of *Pocillopora sp*. **d** Growth of encrusting *Porites sp*. **e** Structural loss of substrate. **f** Overgrowth of fissure in reef surface by calcareous algae. Location of transects noted in each panel, and Fig. 2. Grey shading highlights zones of analysis. Values in **a**–**d** are the mean changes across both years of measurement. Arrows highlight zones of marked change in reef elevation. Results for all transects are contained in Supplementary Figs. 4–7.

eco-geomorphic processes that contribute to reef growth (constructive and destructive). Examination of the point (millimetre-scale) measurements along each CRAF transect provide insights on a number of these key processes. Rates of growth of key calcifying organisms can be determined where point-measurements are co-located with known living cover. For example, nodular calcareous algae achieved growth rates of up to 17 mm.y^{-1} and 21.7 mm.y^{-1} in each year (mean = 19.3 mm.yr^{-1}, Transect 1-J, Figs. 2a and 3a). Transects dominated by encrusting red coralline algae also show incremental increase of ~4.0–6.0 mm.y^{-1} (e.g., Site 1-X1, Figs. 2a, 3b). Growth rates of encrusting corals, as expressed as mean net vertical accretion rates, ranged from up to 11.0 mm.y^{-1} for *Pocillopora sp*. (Site 2-E2, Figs. 2b, 3c) and ~6.0 mm.y^{-1} for encrusting *Porites sp*. (Site 3-X1, Figs. 2c, 3d). The high rates of growth of CCA and corals in this high energy, shallow water (high light) zone are consistent with previous estimates of calcification within the archipelago[40–42] and they also sit within the range of values reported from other reef-building provinces[43–48].

Changes in reef surface topography reveal a highly dynamic surface, with maximum and minimum vertical differences of 138.4 mm y^{-1} and −92.0 mm y^{-1} (Table 1). Of note, variability in surface topography was greatest at sites with higher living calcifier cover and rugosity. Close examination of such high-magnitude changes between years also highlights other process dynamics that affect reef accretion patterns. First, significant losses in vertical structure are identified within years (e.g., up to 57.0 mm, Figs. 2 and 3e) that are likely attributable to physical impact damage in the turbulent wave breaking zone that can promote near instantaneous change in surface elevation. Lower magnitude rates of surface lowering identified at more landward sites may be caused by bioerosion actions of echinoderms[49] and parrot fish[50,51]. Second, marked increases in reef level of up to 120 mm are detected, focused around smaller (cm-scale) fissures in the reef surface (e.g., Figs. 2a, 3f). Such marked increases are attributed to either detrital fill of fissures and/or their closure by lateral expansion of CCA or corals. These mechanisms of reef development have previously been widely recognised in paleo-reconstructions of reef growth, based on the amount of detrital material comprising the reef matrix[9,52], however, our observations reveal the rapid temporal scale that these mechanisms can influence reef development in a contemporary setting.

Functionally, it is the absolute change in reef crest/flat elevation that is most important with respect to the wave dissipation and the wave buffering role of coral reefs, rather than the specific mechanism of change. Our site-specific observations of reef surface development underscore the importance of a suite of reef growth mechanisms that contribute to reef development. In particular, while linear vertical growth of calcifying organisms is a critical factor, other biological and physical processes also contribute to reef development (e.g., detrital infill, rubble sheets, storm deposits)[53]. This entire suite of processes must be considered in assessing future changes in elevation of reefs and their capacity to persist as important wave buffering structures[1].

Results also provide estimates of net calcium carbonate budgets at our reef sites, and which are reef zones that are seldom studied (Fig. 1b), for comparison with studies based on census-based

approaches (G, where $G = CaCO_3$ Kg m^{-2} yr^{-1}). Production rates at the outer reef crest range from 8.51 and 12.51 G (mean 10.39 G). Values are comparable to the upper range of reef production values reported in the Caribbean[54,55]; Indian Ocean[56] and western Pacific[29,30], though these studies focus on forereef environments. Significantly, the high rate measured at the reef crest is also comparable to early estimates of production on outer reef flat surfaces[34,36,57]. Further landward, in the narrow coral-algal zone, carbonate production values range from −1.11 to 4.98 G (across Sites 2 and 3) with a mean value of 2.35 G, also consistent with the values reported from reef flat surfaces[35,57,58]. The algal pavement zone had lower production values ranging between −2.69 and 1.15 G (mean −0.77).

Our results also highlight local-scale variability in reef growth rates specific to eco-geomorphic zones, which can be masked in aggregated reef system analyses. The reef rim at the study location has maintained a positive accretion state. Notably, recent studies from the same atoll have indicated a recent collapse in reef accretion state (to −0.4 mm.yr^{-1}) at depths of 5 m on the forereef of lagoonal systems following a major bleaching event in 2016[37]. This evidence has subsequently been used to infer broader collapse of carbonate budget states in the Maldives and to predict a prolonged period of suppressed budget and reef growth that would promote reef submergence and island instability[4,37]. Our data indicate that in contrast to the fore-reef of lagoonal platforms, the outer algal rim of the ocean reef flat has maintained a productive state within two years of this major bleaching event (~6.6 mm.yr^{-1}), and is consistent with both pre-bleaching estimates[4,20] and with a study showing a positive carbonate production state of a lagoonal reef platform surface shortly after the bleaching event[33]. Collectively these studies highlight the spatial heterogeneity in growth rates that depend on the reef sector and zonal depth under investigation. They also demonstrate that habitat-related responses to climate disturbance vary, and are dependent on ecological community composition of each eco-geomorphic zone. Such findings suggest inferences on morphological and hazard consequences for islands, based on analyses of reef-slope sectors that are of secondary importance to the critical reef crest zone that induces wave breaking, should be made with caution acknowledging the unevenness in reef growth rates between different reef habitat zones.

Here we compare our measured rates of contemporary reef accretion against current and future projections of sea level over the next century (Fig. 4). Significantly the CCA-dominated reef crest accreted at a rate of 6.6 mm.yr^{-1} in each 12-month period (2018–19; 2019–2020). Such growth, exceeds the current rate of sea level change in the archipelago (3.46 ± 0.25 mm.yr^{-1})[59], and is comparable to the RCP 4.5 scenario (6.9 mm.yr^{-1}) but is less than the RCP 8.5 projection (9.6 mm.yr^{-1}), although the variability in accretion rates does span this higher rate of sea level change. Although variable, mean accretion rates at the outer reef flat sites (sites 2 and 3) match current rates of sea level change where there is productive cover, though are less than both the RCP4.5 and RCP8.5 scenarios. Site 4, with low coral-algal and coral cover, currently has no functional accretion capacity and falls below current and future rates of sea level change.

If the observed rates of reef accretion persist, our results suggest that accretion of the reef crest may continue under moderate rates of sea level change. Consequently, the short-term measurements reported here indicate that the reef crest may retain the potential to develop its structure and maintain its function as an effective barrier to incident wave energy. The ability of the algal-dominated reef crest to 'keep pace' with sea level is consistent with geological interpretations of the growth performance of windward reef crests in the Indo-Pacific, that yielded thick algal crusts and dense reef framework (coralline algal facies)[9]. However, observed rates of accretion of the

landward reef flat zones are below the anticipated future rates of sea level change, and the recorded spatial variability in accretion rates suggests broader structural transformations and relative submergence of the central reef flat surface may occur. The implications of such structural change must be considered in revised wave modelling studies to examine island erosion, flooding and vulnerability[7,60–63]. These findings highlight the pressing need for continued measurement of reef flat accretion rates, and expansion of measurements to other representative reef sites.

It is important to recognise a number of spatial and temporal limitations of our data. First, our dataset comprises a small number of sample sites, though ecological surveys indicate they are representative of actively calcifying eco-geomorphic zones on the reef flat at the field site (Methods, Supplementary Note 1). Consequently, extrapolation of findings from this small dataset is constrained. Additional measurement sites within the eco-geomorphic zones in Huvadhoo atoll, and between different reef sites in the Maldives is necessary to support broader extrapolation and robust predictions of future reef growth at the archipelagic scale. Second, our accretion estimates do not incorporate a range of other processes that may also affect reef accretion performance over medium timescales. For example, the dataset was generated across a timeframe of normal wave energy conditions, during which there was an absence of significant storm events (Supplementary Fig. 8). Due to its proximity to the equator storms are infrequent at the field site[59]. However, when such events do occur, they could promote reef damage[64] causing reef development to follow the intermediate disturbance hypothesis of reef accretion punctuated by degradation[65]. In this circumstance, our results may be skewed to higher accretion values than if the negative impact of infrequent storms had influenced our measurement period. However, storms may also generate rubble from the forereef, which if deposited on the reef flat, could promote a step change in reef flat level[53]. Of note, a storm rubble tract is present on the outer reef (Supplementary Fig. 1d) and if this situation were to recur our results may be skewed to lower accretion values due to the absence of storms during the study period. Ongoing monitoring that incorporates such events will be essential to understand how storms impact reef accretion rates; and improve confidence in the extrapolation of our reef accretion rates over the medium-term. Furthermore, as the central reef flat undergoes submergence due to sea-level rise, expansion of productive cover from the CCA/coral zone may enable the broader reef flat, which is currently intertidal, to recolonize and resume vertical growth. The rate of such recolonization and growth will determine the absolute degree of reef flat submergence. Additional environmental stressors are also likely to impact calcification at the reef rim including, ocean acidification, ocean warming, and the magnitude and frequency of bleaching events. As projected by Cornwall[20] such stressors are likely to negatively impact the accretion rates of contemporary reefs and influence the structure and topography of reefs. However, contrary to this view, our data show high rates of growth at the atoll reef algal rim two years after a major bleaching episode in 2016[37]. These measured growth rates are comparable to reported pre-bleaching growth rates[4,20], suggesting that CCA may be an important calcifier that can maintain active vertical growth in the wave-breaking zone following periods of elevated sea surface temperatures. As the CRAF method integrates the suite of processes that result in net changes in reef elevation, we suggest that ongoing monitoring of reef accretion rates will provide a ground-truthed quantitative basis to assess the impact of these additional stressors on medium-term reef growth.

This study demonstrates the value of detailed, site-specific, direct measurements of reef surface topographic change for the study of contemporary and future reef trajectories. The CRAF
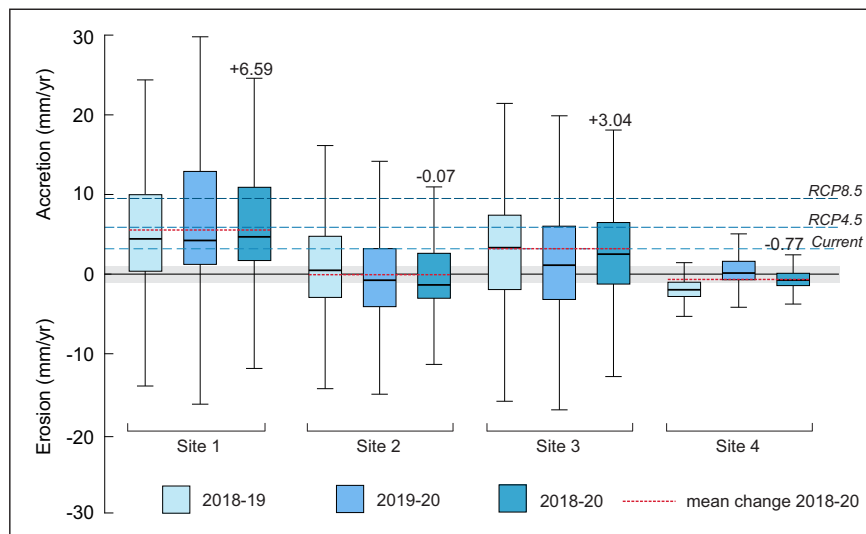
Fig. 4 Comparison of reef accretion rates at outer reef flat sites in Huvadhoo atoll with current and future projections of sea-level rise. Results for each site are presented for each year and the aggregated annual mean across the experimental period. Sea-level rise scenarios presented are the contemporary rate of change in the southern Maldives of 3.46 ± 0.25 mm.y^{-1}, and the global scenarios of RCP 4.5 = 6.9 mm.y^{-1} and RCP 8.5 = 9.6 mm.y^{-1}. Note, rates of change at site four sit within the margin of error of CRAF measurements and indicate no net change. Boxes represent the interquartile range from the 25th to 75th percentiles, horizontal black line is the median, whiskers represent the minimum and maximum values.

method provides valuable and repeatable quantitative measurements of contemporary net reef accretion at a finer temporal and spatial resolution than has previously been reported. The fine-scale resolution of data affords opportunities to examine in detail the process of contemporary reef development and can be used to validate reef budget estimates. Establishment of additional monitoring sites will provide the basis for robust extrapolations of future reef growth and enable issues of scale in future projections to be better resolved. Furthermore, establishment of new sites across different reef regions, and reef types, will provide essential comparative data on contemporary reef growth performance. Ongoing monitoring will also provide verification of projections of physical reef response to a suite of environmental changes[20] and can inform ongoing refinement of models that predict reef growth trajectories, as well as models that resolve the effectiveness of reefs as wave dissipating structures. Thus, the changing character of wave-induced flood and erosion hazard impacts on reef-adjacent island coastlines can be more robustly assessed.

Our method and data provide direct contemporary measures of reef accretion capacity at the shallow reef crest, the zone critical to wave breaking. The results show that the contemporary accretion rate observed during the two-year study period can keep pace with current rates of sea-level rise. While additional measurements and analysis from representative reef regions are necessary to establish a robust global understanding of contemporary and future reef accretion rates, the findings provide the first step in underscoring the importance of focused climate mitigation strategies to minimize rates of sea-level rise to enable coral reefs to maintain relative elevation and therefore continue to afford adjacent shorelines protection from ocean wave energy.

Methods

Field location. This study develops and implements a direct and repeatable approach to measure changes in reef surface topography in the critical reef crest zone that induces wave breaking. Detailed changes in the topography of the reef surface were measured on the southern exposed atoll reef rim of Huvadhoo atoll (0º32' N, 73º17' E), in the southern Maldives archipelago (Supplementary Fig. 1). Huvadhoo is the largest discrete atoll in the archipelago with a reef rim perimeter of 261.4 km and a reef area of 3,279 km^2 [66]. The atoll rim structure rises steeply from oceanic depths >2000 m, terminating at the reef crest near modern sea level (Supplementary Fig. 1c–e). The study examined reef flat growth midway along an

11.4 km long section of the reef rim on the southern and western side of Huvadhoo (Supplementary Fig. 1b, c). This sector of the reef structure varies in width between 0.85 and 1.4 km and the platform provides the basement for 11 vegetated reef islands.

The experimental site is the outer reef flat seaward of the vegetated island Keleihutta (Supplementary Fig. 1c). The topography of the reef and reef flat at this location is typical of the ocean reef morphology around the atoll, and is also similar to other sea level constrained atoll rim reefs throughout the Indo-Pacific. The upper forereef, between depths of 0–15 m is characterized by a well-defined spur and groove structure (Supplementary Fig. 1c, d). The forereef has a steep gradient that terminates in a sharp break in slope at the reef crest at an elevation of −0.52 m below mean sea level (MSL). The reef flat surface is near horizontal ranging in elevation from −0.46 to −0.41 m below MSL on the outer reef flat (100 m section landward of the reef crest) and between −0.41 and −0.25 m MSL on the central to inner reef flat. Of note, a coral cobble/boulder tract comprising clasts up 0.5 m in diameter is located on the outer reef flat. Its seaward edge begins approximately 45 m landward of the reef crest, reaching an elevation of −0.09 m MSL (Supplementary Fig. 1c–e). This boulder tract extends approximately 30–35 m across the reef flat as a contiguous unit, beyond which cobble tongues extend further across the reef surface and overly the coral-algal pavement (Supplementary Fig. 1d). The intertidal reef flat acts as an effective buffer to incident ocean wave energy, reducing energy by 90% across the reef crest (Supplementary Fig. 2).

Oceanographic processes. The ocean wave climate of southern Huvadhoo is influenced by local wave processes generated by seasonal monsoon winds, periodic storms and long period swell waves generated by large low-pressure systems that originate in the Southern Ocean[59,67]. A seasonal distinction can be made in the wave climate, with lower swell and offshore winds at the study site typically persisting during the dry season (between December and February), and a mixture of onshore wind-driven waves and larger long period swell during the wet season (between April and September) (Supplementary Fig. 8). Significant wave height offshore of Huvadhoo is typically just over 1 m during the dry season and ~1.95 m during the wet season. However, there can be significant variability in Hs values about the mean with maximum monthly Hs values ranging from ~2 m in the dry season to ~3.8 m in the wet season respectively. Daily average Hs values throughout the experimental period indicates the wave climate was consistent with long-term trends with maximum average daily Hs values peaking at ~3.2 m (Supplementary Fig. 8). The field site is located close to the equator and consequently, is not affected by frequent extreme wave events. However, larger storms do infrequently occur[59], that can flood nearby islands, though no extreme events impacted the site during the experimental period.

Monthly mean sea surface temperatures in the Maldives range from 28.0 to 29.7 ºC[68]. However, the archipelago has been subject to a number of coral bleaching events associated with sustained elevated SSTs in excess of 30.9 ºC in 1987/88, 1998 and most recently in 2016[37]. Peak SSTs during these events exceed 32.5 ºC which has been reported to have had a major impact on the living cover of corals across the archipelago[37,38].

Analysis of sea level records since 1987 from Gan in the southern Maldives[59] indicates that sea level in the southern archipelago has increased at a mean rate of 3.46 ± 0.25 mm.y^{-1}. Interannual oscillations in mean sea level (MSL), influenced by climate phenomenon such as ENSO and the Indian Ocean Dipole (IOD) are also present in tide gauge measurements with an amplitude in the order of 0.2 m. The atoll is subject to a semi-diurnal tidal regime with a spring tide range of 0.96 m with a pronounced diurnal inequality[59]. Of relevance to this study, sea-level records from Gan show a pronounced sea-level fluctuation between 2018 and 2020 (Supplementary Fig. 9). During the study sea-level in the southern Maldives was typically 20–50 mm above MSL but fluctuated by 200 mm, peaking at 150 mm above MSL in July 2019 (150 mm above MSL; Supplementary Fig. 9). This peak in sea level was associated with a strong positive IOD index.

Experimental sites. Four experimental sites were established across the first 65 m of reef surface from the reef crest (Fig. Supplementary 1c–e) to capture transitions in the eco-morphological characteristics of the outer reef flat. Eco-geomorphic characteristics were determined through a combination of topographic surveys (Supplementary Fig. 1e), field observations, and ecological surveys (Supplementary Note 1 and Supplementary Tables 1 and 2). Four distinctive zones were differentiated. The high energy reef crest (outer 20 m) where the cover of calcifying organisms is dominated by CCA (30.8% cover) with encrusting corals (14% cover); the outer reef flat which has CCA (32.9%) and a higher prevalence of corals (27.9%); a distinctive and narrow boulder tract (Supplementary Fig. 1d, e) with less than 5% cover of calcifying organisms; and, the coral pavement zone that characterises the central reef flat where the cover of calcifying organisms is low (CCA ~3.1% and corals ~8.5%). Experimental sites were established at random on the outer reef crest, the outer reef flat (two sites), and reef pavement zones. Due to gross rugosity characteristics a site was not established in the boulder tract.

Coral reef accretion frame measurements. At each site measurements were obtained using a purpose-built coral reef accretion frame (CRAF) designed to enable repeatable millimetre-scale measurements of reef surface elevation from a fixed and relocatable horizontal reference plane across 0.25 m^2 plots (Fig. 5). At each measurement site a plot was established comprising four bolts, fixed vertically into the reef substrate in a 600×600 mm square. Bolts were positioned and fixed to ensure a level platform for measurements across each plot. Two bars are placed, in parallel, on top of nuts fixed on bolts, to form a horizontal reference plane. Each bar has 57 grooves at 10 mm spacings. A measuring platform, positioned perpendicular to the horizontal bars, locks into the grooves in each bar. An array of 99 vertical measuring rods (500 m long by 1.5 mm in width), are spaced at 5 mm intervals along the measuring platform.

In this study seven transects were measured from the horizontal frame at each site. Once a transect position is established, each rod is lowered through holes in the measuring platform until contact is made with the reef surface. To capture the data, a graduated scale was placed behind the measurement rods (protruding above the measuring bar) and photographed to record the height of rods above the reef surface along each line (Fig. 5c). Photographs were taken with known control points to allow rectification of images. Images were analysed digitally in a georeferenced framework to measure pin elevation and reconstruct the topography of the reef surface underneath each set of pin measurements (Fig. 6). Photographs were rectified and imported into the Matlab function *grabit.m*.[69]. Within the *grabit.m* function the image was calibrated to a known scale (Fig. 6a). Individual points were subsequently digitized (Fig. 6b). Digitising precision is estimated at 0.5 mm and error is estimated at $\pm$ 0.3 mm, calculated as the mean absolute error between repeat digitising of an individual line. Digitised points were saved for each measurement and transformed to a common datum in relation to the top of the measurement platform to reconstruct the topography of the reef surface. In each plot, measurements were made along 7 equidistant lines, totalling 693 measurements per site.

CRAFs were installed in February 2018 and measured to provide the baseline topography of each measurement line. Measurements were repeated in February 2019 and 2020 providing two complete annual cycles of reef surface change. Reduction of data to the same horizontal datum provides a basis to detect elevation changes of the reef surface at each location (mm.y^{-1}). Point specific changes were aggregated to yield the mean and range of topographic changes on each transect. Values were also aggregated to the plot scale to generate mean values of surface change at each site (mm.y^{-1}).

Measurement replication and error. To test the error associated with the measurement technique 10 repeat measurements were made along one transect line involving re-establishment of the measurement frame on each occasion (Fig. 7). This approach incorporated errors including the repositioning of the reference frame between measurement periods, and errors associated with rectification of images. Based on the square root of the sum of squares of each individual measurement error the data indicates that the CRAF measurement error is $\pm$ 1.07 mm. Consequently, measurements that sit within this margin of error are considered to reflect no detectable change in the reef flat surface.

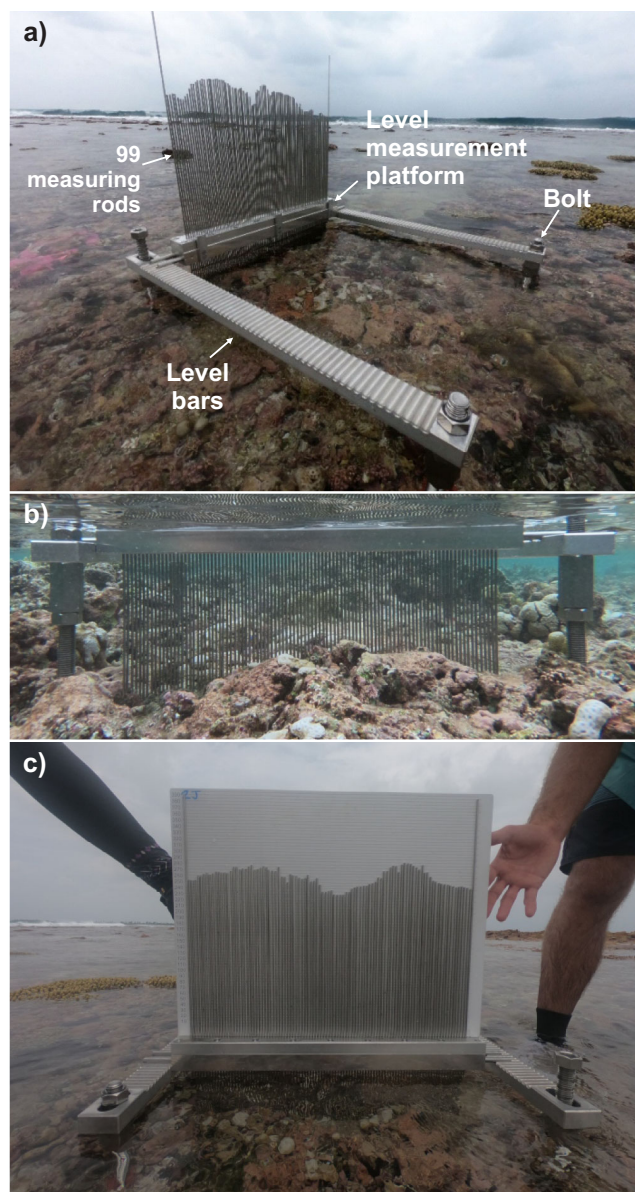**Fig. 5 Coral Reef Accretion Frame (CRAF) setup and measurement system. a** Components of the CRAF at Site 2 on the Keleihutta outer reef flat. **b** Below waterline view of measurement rods defining the reef flat topography. **c** Image of graduated back board used to take in situ images of the reef surface topography beneath the horizontal reference datum.

Statistical analysis. Statistical analyses were performed using the software package PAST, Version 4.02[70]. Assumptions for the tests applied were assessed by examining the data for normality, and if the assumptions were not met, a non-parametric test was substituted. Data were not transformed.

Inter-site differences in total reef elevation change (mm) for the two-year observational period (2018–2020) were analysed by site using a one-way Kruskal-Wallis test because the assumptions of parametric ANOVA were not met (the data were not normally distributed). When differences between site were significant, a post hoc Dunn test with Bonferroni adjustment method were used.

Estimates of reef productivity. The CRAF method yields net changes in reef surface elevation (growth) that integrates the suite of reef growth and destruction processes. The study compares net productivity rates with previous studies based on census-based reef budget approaches that yield net values of G (Kg.m^{-2}.yr^{-1})[28]. To produce comparable G values, net reef growth values from CRAF measurements (mm^{-2}.yr^{-1}) were converted to a known volume of growth (m^{-3}.m^{-2}.yr^{-1}) and converted to a weight of production using a density value of cacifiers using the
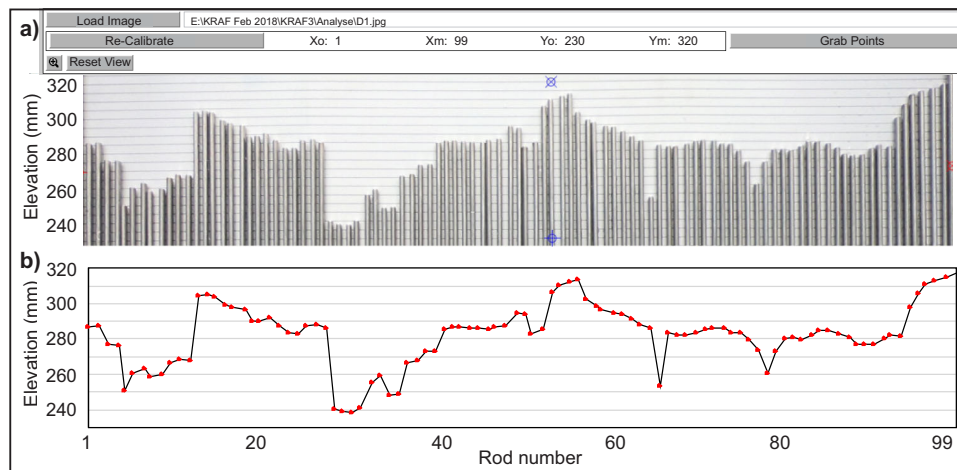
Fig. 6 Overview of steps in capturing the digital data from the CRAF. a Images are rectified and placed in a X-Y scale using the Matlab application *grabit.m*. **b** Each rod is digitized to create X-Y points and reconstruct the topography of the reef surface.
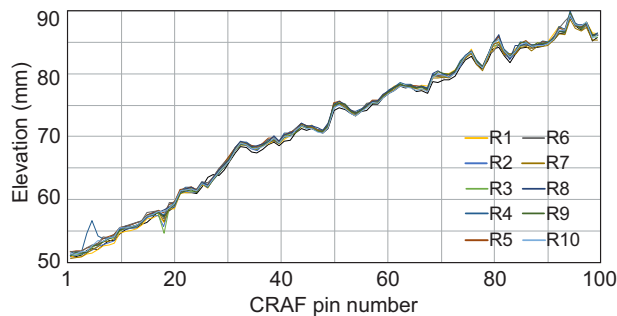

Fig. 7 Results of repeat measurements along transect line D4 at CRAM site 4 to evaluate instrument repositioning errors. Location of site shown in Supplementary Fig. 1d.

following equation:

$$Net\ production\ rate\ G = (VA_{CF}/1000) \times D_i$$

Where G is production in kg $CaCO_3$ m^{-2}.y^{-1}, VA_{CF} is net vertical reef accretion in mm.m^2.y^{-1}, and D_i is density of calcifiers (kg.m^3). This analysis adopted a mean density value of 1,576 kg.m^3 as the mid-range of values of the ReefBudget method[28] and those established from the Maldives[40].

Comparison of measured rates of reef accretion with rates of sea-level rise. We compare the measured rates of reef accretion at the reef crest and outer reef flat zones against recently observed and future projected changes in sea level. Specifically, we compare rates of reef accretion against the current local rate of sea level change (3.46 ± 0.25 mm.y^{-1})[59] and against the projected rates of sea-level rise to 2100 using the RCP4.5 and RCP8.5 scenarios[71,72].

Data availability
Data generated from coral reef monitoring sites in this study are available at https://doi.org/10.5281/zenodo.4321416.

References
1. Ferrario, F. et al. The effectiveness of coral reefs for coastal hazard risk reduction and adaptation. *Nat. Commun.* **5**, 3794 (2014).
2. Graham, N. A. J., Jennings, S., MacNeil, M. A., Mouillet, D. & Wilson, S. K. Predicting climate-driven regime shifts versus rebound potential in coral reefs. *Nature.* **518**, 94–97 (2015).
3. Beck, M. W. et al. The global flood protection savings provided by coral reefs. *Nat. Commun.* **9**, 2186 (2018).
4. Perry, C. T. et al. Loss of coral reef growth capacity to track future increases in sea level. *Nature.* **558**, 396–400 (2018).
5. Reguero, B. G. et al. The value of US coral reefs for flood risk reduction. *Nat. Sustain.* **4**, 688–698 (2021).
6. Tuck, M., Kench, P. S., Ford, M. R. & Masselink, G. Wave overwash processes provide mechanism for reef island to keep up with sea level rise. *Geology.* **47**, 803–806 (2019).
7. Beetham, E. & Kench, P. S. A global tool for predicting future wave-driven flood trajectories on atoll islands. *Nat. Commun.* **9**, 3997 (2018).
8. Perry, C. T., Spencer, T. & Kench, P. Carbonate budgets and reef production states: A geomorphic perspective on the ecological phase-shift concept. *Coral Reefs.* **27**, 853–866 (2008).
9. Montaggioni, L. F. History of Indo-Pacifc coral reef systems since the last glaciation: Development patterns and controlling factors. *Earth Sci. Rev.* **71**, 1–75 (2005).
10. Storlazzi, C. D., Elias, E., Field, M. E. & Presto, M. K. Numerical modelling of the impact of sea-level rise on fringing coral reef hydrodynamics and sediment transport. *Coral Reefs* **30**, 83–96 (2011).
11. Quataert, E. et al. The influence of coral reefs and climate change on wave-driven flooding of tropical coastlines. *Geophys. Res. Lett.* **42**, 6407–6415 (2015).
12. Alvarez-Filip, L., Dulvy, N. K., Gill, J. A., Côte, I. M. & Watkinson, A. R. 2009. Flattening of Caribbean coral reefs: Region-wide declines in architectural complexity. *Proc. R. Soc. B* **276**, 3019–3025 (2009).
13. Sheppard, C., Dixon, D. J., Gourlay, M., Sheppard, A. & Payet, R. Coral mortality increases wave energy reaching shores protected by reef flats: Examples for the Seychelles. *Estuar. Coast Shelf Sci.* **64**, 223–234 (2005).
14. Perry, C. T. & Alvarez-Filip, L. Changing geo-ecological functions of coral reefs in the Anthropocene. *Funct. Ecol.* https://doi.org/10.1111/1365-2435.13247 (2018).
15. Moss, R. H. et al. The next generation of scenarios for climate change research and assessment. *Nature* **463**, 747–756 (2010).
16. Church, J. A. et al. in Climate Change 2013: The Physical Science Basis (ed. Stocker, T. F. et al.) Ch. 13 Cambridge Univ. Press (2013).
17. Perry, C. T. et al. Caribbean-wide decline in carbonate production threatens coral reef growth. *Nat. Commun.* **4**, 1402–1409 (2013).
18. Hughes, T. P. et al. Spatial and temporal patterns of mass bleaching of corals in the Anthropocene. *Science* **359**, 80–83 (2018).
19. Hughes, T. P. et al. Global warming impairs stock–recruitment dynamics of corals. *Nature* **568**, 387–390 (2019).
20. Cornwall, C. E. et al. Global declines in coral reef calcium carbonate production under ocean acidification and warming. *Proc. Nat, Acad. Sci.* **118**, 20e2015265118 (2021).
21. Levermann, A. et al. The multimillennial sea-level commitment of global warming. *Proc. Nat. Acad Sci.* **110**, 13745–13750 (2013).
22. Kopp, R. E. et al. Probabilistic 21st and 22nd century sea-level projections at a global network of tide gauge sites. *Earths Future* **2**, 383–406 (2014).
23. Rasmussen, D. J. et al. Extreme sea level implications of 1.5ºC, 2ºC and 2.5ºC temperature stabilization targets in the 21st and 22nd century. *Environ. Res. Lett.* **13**, 034040 (2018).

24. Kench, P. S., Perry, C. T. & Spencer, T. Coral Reefs. Chapter 7 in Slaymaker O., Spencer, T and Embleton-Haman, C. (ed.) *Geomorphology and Global Environmental Change*, Cambridge University Press, Cambridge, p. 180–213 (2009).

25. Dullo, W. C. Coral growth and reef growth: A brief review. *Facies.* **51**, 33–48 (2005).

26. Roff, G., Zhao, J.-X. & Pandolfi, J. M. Rapid accretion of inshore reef slopes from the central Great Barrier Reef during the late Holocene. *Geology.* **43**, 343–346 (2015).

27. Roff, G. Reef accretion and coral growth rates are decoupled in Holocene reef frameworks. *Mar. Geol.* **419**, 106065 (2020).

28. Perry, C. T. et al. Estimating rates of biologically driven coral reef framework production and erosion: A new census-based carbonate budget methodology and applications to the reefs of Bonaire. *Coral Reefs.* **31**, 853–868 (2012).

29. Van Woesik, R. & Cacciapaglia, C. W. Keeping up with sea-level rise: Carbonate production rates in Palau and Yap, western Pacific Ocean. *PLoS ONE.* **13**, e0197077 (2018).

30. Van Woesik, R. & Cacciapaglia, C. W. Carbonate production of Micronesian reefs suppressed by thermal anomalies and Acanthaster as sea-level rises. *PLoS ONE.* **14**, e0224887 (2019).

31. Perry, C. T., Smithers, S. G. & Gulliver, P. Rapid vertical accretion on a 'young' shore-detached turbid zone reef: Offshore Paluma Shoals, central Great Barrier Reef, Australia. *Coral Reefs.* **32**, 1143–1148 (2013).

32. Kench, P. S. & Brander, R. W. Wave processes on coral reef flats: implications for reef geomorphology using Australian case studies. *J. Coast. Res.* **22**, 209–223 (2006).

33. Ryan, E. J., Hanmer, K. & Kench, P. S. Positive reef flat carbonate budget after bleaching event on a southern Maldivian reef attributed to dominance of massive corals. *Sci. Rep.* **9**, 6515 (2019).

34. Chave, K. E., Smith, S. V. & Roy, K. J. Carbonate production by coral reefs. *Mar. Geol.* **12**, 123–140 (1972).

35. Smith, S. V. & Kinsey, D. W. Calcium carbonate production, coral reef growth, and sea level change. *Science.* **194**, 937–939 (1976).

36. Kinsey, D. W. Standards of performance in coral reef primary production and carbon turnover. In: Barnes, D. J. (Ed.) *Perspectives on Coral Reefs.* Brian Clouster Publ., Manuka, Australia, pp. 209–220 (1983).

37. Perry, C. T. & Morgan, K. M. Bleaching drives collapse in reef carbonate budgets and reef growth potential on southern Maldives reefs. *Sci. Rep.* **7**, 40581 (2017).

38. Cowburn, B., Moritz, C., Grimsditch, G. & Solandt, J. L. Evidence of coral bleaching avoidance, resistance and recovery in the Maldives during the 2016 mass-bleaching event. *Mar. Ecol. Prog. Ser.* **626**, 53–67 (2019).

39. Adey, W. H. & Vassar, J. M. Colonization, succession and growth rates of tropical crustose coralline algae (Rhodophyta, Cryptonemiales). *Phycologia.* **14**, 55–69 (1975).

40. Morgan, K. M. & Kench, P. S. Skeletal extension and calcification of reef-building corals in the central Indian Ocean. *Mar. Env. Res.* **81**, 78–82 (2012).

41. Morgan, K. M. & Kench, P. S. Carbonate production rates of encruster communities on a lagoonal patch reef: Vabbinfaru reef platform. *Maldives. Mar. Fresh. Res.* **65**, 720–726 (2013).

42. Morgan, K. M. & Kench, P. S. New rates of Indian Ocean carbonate production by encrusting coral reef calcifiers: Periodic expansions following disturbance influence reef-building and recovery. *Mar. Geol.* **390**, 72–79 (2017).

43. Agegian, C. R. Growth of the branched coralline alga, *Porolithon gardineri* (Foslie), in the Hawaiian archipelago. In *Proc. 4th Int. Coral Reef Symp.* 419–423 (1981).

44. Mallela, J. Coral reef encruster communities and carbonate production in cryptic and exposed coral reef habitats along a gradient of terrestrial disturbance. *Coral Reefs.* **26**, 775–785 (2007).

45. Matsuda, S. Succession and growth rates of encrusting crustose coralline algae (Rhodophyta, Cryptonemiales) in the upper fore-reef environment off Ishigaki Island, Ryukyu Islands. *Coral Reefs.* **7**, 185–195 (1989).

46. Pari, N. et al. Bioerosion of experimental substrates on high islands and on atoll lagoons (French Polynesia) after two years of exposure. *Mar. Ecol. Prog. Ser.* **166**, 119–13 (1998).

47. Stearn, C., Scoffin, T. & Martindale, W. Calcium carbonate budget of a fringing reef on the west coast of Barbados. Part I. Zonation and productivity. *Bull. Mar. Sci.* **27**, 479–510 (1977).

48. Steneck, R. S. & Adey, W. H. The role of environment in control of morphology in *Lithophyllumcongestum*, a Caribbean algal ridge builder. *Bot. Mar.* **19**, 197–216 (1976).

49. Bak, R. P. M. Patterns of echinoid bioerosion in two Pacific coral reef lagoons. *Mar. Ecol. Prog. Ser.* **66**, 267–272 (1990).

50. Morgan, K. M. & Kench, P. S. Parrotfish erosion underpins reef growth, sand talus development and island-building in the Maldives. *Sed. Geo.* **341**, 50–57 (2016).

51. Yarlett, R. T., Perry, C. T., Wilson, R. W. & Philpot, K. E. Constraining species-size class variability in rates of parrotfish bioerosion on Maldivian coral reefs: implications for regional-scale bioerosion estimates. *Mar. Ecol. Prog. Ser.* **590**, 155–169 (2018).

52. Hubbard, D. K. & Dullo, W. C. The changing face of reef building. In *Coral Reefs at the Crossroads*, (eds Hubbard, D. K., Rogers, C. S., Lipps, J. H., Stanley, G. D.) p.127–153, (2016).

53. Blanchon, P., Jones, B. & Kalbfleisch, W. Anatomy of a fringing reef around Grand Cayman; storm rubble, not coral framework. *J. Sed. Res.* **67**, 1–16 (1997).

54. Perry, C. T. et al. Changing dynamics of Caribbean reef carbonate budgets: emergence of reef bioeroders as critical controls on present and future reef growth potential. *Proc. R. Soc. B.* **281**, 20142018 (2014).

55. Perry, C. T. et al. Regional-scale dominance of non-framework building corals on Caribbean reefs affects carbonate production and future reef growth. *Glob. Change Biol.* **21**, 1153–1164 (2015).

56. Perry, C. et al. Remote coral reefs can sustain high growth potential and may match future sea-level trends. *Sci Rep* **5**, 18289 (2015).

57. Kinsey, D. W. The Pacific/Atlantic reef growth controversy. *Proc. 4th Int. Coral Reef Symp.* Manila **1**, 493–498 (1981).

58. Hart, D. E. & Kench, P. S. Carbonate production of an emergent reef platform, Warraber Island, Torres Strait, Australia. *Coral Reefs* **26**, 53–68 (2006).

59. Wadey, M., Brown, S., Nicholls, R. J. & Haigh, I. Coastal flooding in the Maldives: an assessment of historic events and their implications. *Nat. Hazards* **89**, 131–159 (2017).

60. Beetham, E., Kench, P. S. & Popinet, S. Future reef growth can mitigate physical impacts of sea-level rise on atoll islands. *Earth's Future* **5**, https://doi.org/10.1002/2017EF000589 (2017).

61. Harris, D. L. et al. Coral reef structural complexity provides important coastal protection from waves under rising sea levels. *Sci. Adv.* **4**, eaao4350 (2018).

62. Storlazzi, C. D. et al. Most atolls will be uninhabitable by the mid-21st century because of sea-level rise exacerbating wave-driven flooding. *Sci. Adv.* **4**, eaap9741 (2018).

63. Masselink, G., McCall, R., Beetham, E., Kench, P. & Storlazzi, C. Role of future reef growth on morphological response of coral reef islands to sea-level rise. *J. Geophys. Res., Earth Surf.* **126**, e2020JF005749 (2021).

64. Puotinen, M. et al. Towards modelling the future risk of cyclone wave damage to the world's coral reefs. *Glob. Change Biol.* **26**, 4302–4315 (2020).

65. Connell, J. H. Diversity in tropical rain forests and coral reefs. *Science.* **199**, 1302–1310 (1978).

66. Naseer, A. & Hatcher, B. G. Inventory of the Maldives coral reefs using morphometrics generated from Landsat ETM+ imagery. *Coral Reefs* **23**, 161–168 (2004).

67. Amores, A. et al. Coastal Flooding in the Maldives Induced by Mean Sea-Level Rise and Wind-Waves: From Global to Local Coastal Modelling. *Front. Mar. Sci.* **8**, 665672.

68. NOAA Coral Reef Watch site (http://coralreefwatch.noaa.gov/vs/gauges/maldives.php).

69. Jiro, GRABIT (https://www.mathworks.com/matlabcentral/fileexchange/7173-grabit), MATLAB Central File Exchange. Retrieved February 12, (2018).

70. Hammer, O., Harper, D. A. T. & Ryan, P. D. 2001. PAST: Paleontological statistics software package for education and data analysis. *Palaeontol. Electron.* **4**, 9 (2001).

71. Slangen, A. B. A. et al. Projecting twenty-first century regional sea-level changes. *Clim. Change.* **124**, 317–332 (2014).

72. Carson, M. et al. Coastal sea level changes, observed and projected during the 20th and 21st century. *Clim. Change.* **134**, 269–281 (2016).

Author contributions

P.K. conceived the project; P.K., E.B., T.T., K.M., S.O, and R.M. undertook fieldwork; E.B., T.T., and P.K. undertook data analysis; P.K. led paper development and interpretation and all authors contributed to paper revision and figures.

Competing interests

The authors declare no competing interests.

Additional information

Supplementary information The online version contains supplementary material available at https://doi.org/10.1038/s43247-021-00338-w.

Correspondence and requests for materials should be addressed to Paul S. Kench.

Peer review information *Communications Earth & Environment* thanks Curt Storlazzi and the other, anonymous, reviewer for their contribution to the peer review of this work. Primary Handling Editors: Clare Davis. Peer reviewer reports are available.

Reprints and permission information is available at http://www.nature.com/reprints

Publisher's note Springer Nature remains neutral with regard to jurisdictional claims in published maps and institutional affiliations.